PCP
PLANT & CELL PHYSIOLOGY

Hydrogen Sulfide Regulates the Cytosolic/Nuclear Partitioning of Glyceraldehyde-3-Phosphate Dehydrogenase by Enhancing its Nuclear Localization

Angeles Aroca[1], Markus Schneider[2], Renate Scheibe[2], Cecilia Gotor[1] and Luis C. Romero[1,*]

[1]Instituto de Bioquímica Vegetal y Fotosíntesis, Consejo Superior de Investigaciones Científicas y Universidad de Sevilla, 41092 Sevilla, Spain
[2]Department of Plant Physiology, Osnabrück University, D-49069 Osnabrück, Germany
*Corresponding author: E-mail, lromero@ibvf.csic.es; Fax, +34-954-461065.
(Received March 3, 2017; Accepted April 13, 2017)

Hydrogen sulfide is an important signaling molecule comparable with nitric oxide and hydrogen peroxide in plants. The underlying mechanism of its action is unknown, although it has been proposed to be *S*-sulfhydration. This post-translational modification converts the thiol groups of cysteines within proteins to persulfides, resulting in functional changes of the proteins. In *Arabidopsis thaliana*, *S*-sulfhydrated proteins have been identified, including the cytosolic isoforms of glyceraldehyde-3-phosphate dehydrogenase GapC1 and GapC2. In this work, we studied the regulation of sulfide on the subcellular localization of these proteins using two different approaches. We generated GapC1–green fluorescent protein (GFP) and GapC2–GFP transgenic plants in both the wild type and the *des1* mutant defective in the L-cysteine desulfhydrase DES1, responsible for the generation of sulfide in the cytosol. The GFP signal was detected in the cytoplasm and the nucleus of epidermal cells, although with reduced nuclear localization in *des1* compared with the wild type, and exogenous sulfide treatment resulted in similar signals in nuclei in both backgrounds. The second approach consisted of the immunoblot analysis of the GapC endogenous proteins in enriched nuclear and cytosolic protein extracts, and similar results were obtained. A significant reduction in the total amount of GapC in *des1* in comparison with the wild type was determined and exogenous sulfide significantly increased the protein levels in the nuclei in both plants, with a stronger response in the wild type. Moreover, the presence of an *S*-sulfhydrated cysteine residue on GapC1 was demonstrated by mass spectrometry. We conclude that sulfide enhances the nuclear localization of glyceraldehyde-3-phosphate dehydrogenase.

Keywords: Arabidopsis • *des1* mutant • GFP fusion protein • Mass spectrometry • Nuclei-enriched extract • *S*-sulfhydration.

Abbreviations: ACN, acetonitrile; CaMV, *Cauliflower mosaic virus*; DES, L-cysteine desulfhydrase; GapC, cytosolic glyceraldehyde-3-phosphate dehydrogenase; GAPDH, glyceraldehyde-3-phosphate dehydrogenase; GFP, green fluorescent protein; H_2O_2, hydrogen peroxide; H_2S, hydrogen sulfide; LC, liquid chromatography; MS/MS, tandem mass spectrometry; NaHS, sodium hydrosulfide; NO, nitric oxide; OASA1, *O*-acetylserine(thiol)lyase isoform A1; PMSF, phenylmethylsulfonyl fluoride; PRM, parallel reaction monitoring; RT–PCR, reverse transcription–PCR; TFA, trifluoroacetic acid.

Introduction

Recently, a change in the concept of hydrogen sulfide (H_2S) as a toxic molecule to a regulator of essential life processes has occurred, and it is referred to as the third gasotransmitter in animal cells, as important as nitric oxide (NO) and carbon monoxide (CO) (Gadalla and Snyder 2010, Wang 2012). Numerous plant biological studies have also elevated sulfide to the same level of importance as other signaling molecules, such as NO and hydrogen peroxide (H_2O_2) (Garcia-Mata and Lamattina 2013, Calderwood and Kopriva 2014).

The main source of sulfide for plants are the chloroplasts where it is produced in the sulfate reduction stage of the photosynthetic assimilation pathway (Takahashi et al. 2011), and it was thought to reach the cytosol by diffusion through the chloroplast membranes. However, H_2S dissociates in aqueous solution into H^+ and HS^-, the latter subsequently dissociates into H^+ and S^{2-}, and these ionized forms do not permeate membranes (Kabil and Banerjee 2010). At the basic pH of the chloroplasts (Wu and Berkowitz 1992), these predominant ionic forms are unable to cross the chloroplast envelope. Similarly, the sulfide produced in mitochondria by the detoxification of cyanide (Alvarez et al. 2012c) is predominantly present in ionic forms due to the basic stromal pH (Santo-Domingo and Demaurex 2012). Therefore, the source of sulfide in the cytosol has been proposed to be of biochemical origin related to cysteine metabolism.

The L-cysteine desulfhydrase DES1 enzyme located in the cytosol in Arabidopsis plants catalyzes the desulfuration of cysteine to sulfide, ammonia and pyruvate, and it has been established to be responsible for the release of H_2S in this cell compartment (Alvarez et al. 2010, Gotor et al. 2010). Detailed characterization of DES1-deficient mutants (*des1*) revealed its function in the generation of sulfide in the cytosol for signaling (Romero et al. 2013, Romero et al. 2014, Gotor et al. 2015). Thus, *DES1* mutation reduces the total leaf endogenous H_2S concentration and affects important plant processes, such as plant

Plant Cell Physiol. 58(6): 983–992 (2017) doi:10.1093/pcp/pcx056, Advance Access publication on 24 April 2017, available online at www.pcp.oxfordjournals.org

responses to abiotic stress conditions, plant immunity, regulation of leaf senescence, progress of autophagy and modulation of ABA-dependent stomatal closure (Alvarez et al. 2010, Alvarez et al. 2012a, Alvarez et al. 2012b, Scuffi et al. 2014, Laureano-Marin et al. 2016).

The underlying mechanisms of the action of sulfide and specific targets are still poorly understood in mammals and plants. Different models have been proposed based on the nucleophilic properties of the molecule H_2S, although recent advances highlight as the most likely mechanism the post-translational modification of protein cysteine residues. This process is called *S*-sulfhydration or persulfidation, and consists of the conversion of the thiol group (–SH) into a persulfide group (–SSH), resulting in functional changes in enzymatic activities, structures and subcellular localizations of the target proteins (Mustafa et al. 2009, Mustafa et al. 2011, Paul and Snyder 2012).

To date, several proteins have been identified as targets for this post-translational modification of the cysteine residue, including glyceraldehyde-3-phosphate dehydrogenase (GAPDH). Numerous publications investigating the *S*-sulfhydration of GAPDH and its regulation have been highlighted in recent years due to the importance of this protein in diverse biological functions, in addition to its classical glycolytic role. These include its participation in mRNA regulation, DNA replication, endocytosis or regulation of apoptosis (Sirover 2011, Henry et al. 2015, White and Garcin 2016). Mammalian GAPDH was first described as an *S*-sulfhydrated protein at Cys150 and this modification results in an increase in enzymatic activity in mice (Mustafa et al. 2009). However, in a recent study, polysulfide treatment resulted in the *S*-sulfhydration of GAPDH but a decrease in enzymatic activity (Jarosz et al. 2015). Furthermore, the *S*-sulfhydration of GAPDH promotes its binding to the E3-ubiquitin ligase Siah1, thereby augmenting degradation of the scaffolding molecule PSD95 (Mir et al. 2014).

There are several isoforms of GAPDH in plants that exhibit differential subcellular localization, and several non-metabolic functions have been described for these isoforms. The cytosolic isoform (GapC) has also been detected in the nucleus and plays roles in mRNA regulation, transcriptional activation and apoptosis depending on its nuclear translocation outcome (Ortiz-Ortiz et al. 2010). However, the mechanism of nuclear translocation in plants is still unknown.

Very recently, *S*-sulfhydration has been demonstrated endogenously in Arabidopsis using a modified biotin switch method previously used in mammals, and a total of 106 *S*-sulfhydrated proteins were identified, including the cytosolic GapC. Immunoblot and enzyme activity analyses showed that the sulfide added through this modification reversibly regulates the function of the plant proteins in a manner similar to that described in mammalian systems (Aroca et al. 2015).

Post-translational modifications on catalytic cysteines in Arabidopsis GapC are important for its regulation, function and subcellular localization. GapC undergoes *S*-nitrosylation, *S*-glutathionylation, *S*-sulfhydration, *S*-sulfenylation and other modifications all occurring on the same cysteine residue (Bedhomme et al. 2012, Waszczak et al. 2014, Aroca et al. 2015). In this study, we investigated the effects of H_2S on the subcellular localization of Arabidopsis GapC through *S*-sulfhydration of this protein.

Results

GAPDH was identified and widely characterized as a protein that undergoes post-translational modification by *S*-sulfhydration on its cysteine residues (Mustafa et al. 2009, Zhang et al. 2014), and this modification alters the catalytic activities of the enzyme (Aroca et al. 2015, Jarosz et al. 2015). Because GAPDH isoforms GapC1 and GapC2 are translocated to the nucleus (Holtgrefe et al. 2008, Vescovi et al. 2013), we studied the effects of decreased sulfide production in the *des1* mutant on cytosolic/nuclear partitioning.

To elucidate the subcellular localization of GapC in Arabidopsis, *green fluorescent protein* (*GFP*)-fused constructs with *GapC1* and *GapC2* cDNAs were created under a *35S-CaMV* (*Cauliflower mosaic virus*) promoter and used to obtain stable *GapC1–GFP* and *GapC2–GFP* transgenic plants on both the wild-type and *des1* backgrounds. Fluorescent signals were analyzed with a confocal laser scanning microscope in leaves from 30-day-old plants.

Both GapC–GFP chimeric proteins, GapC1–GFP and GapC2–GFP, were detected in the cytoplasm and the nucleus reproducibly in wild-type background transgenic plants (**Fig. 1A, C**). However, GapC1–GFP and GapC2–GFP chimeric proteins were primarily localized in the cytoplasm cell periphery and the perinuclear region in *des1* mutant overexpression lines, with reduced nuclear localization compared with wild-type plants (**Fig. 1B, D**). Because *des1* mutant plants show a 30% reduction in endogenous sulfide compared with wild-type plants (Alvarez et al. 2012b), our results may suggest that sulfide induces the nuclear localization of the GapC enzymes. To corroborate this observation, we analyzed the effects of exogenous sulfide treatment on GapC–GFP localization in leaves from plants grown under physiological conditions, which were treated exogenously for 2 h with 200 μM sodium hydrosulfide (NaHS). Transgenic wild-type background plants did not exhibit any significant changes in GapC1–GFP and GapC2–GFP localization due to the sulfide treatment; they were localized in the cytoplasm and the nucleus (**Fig. 1E, G**). However, chimeric proteins were significantly detected in the nucleus and the cytoplasm in mutant *des1* transgenic plants that were sulfide treated (**Fig. 1F, H**). Nuclear staining was performed with SYTO® Blue45 on the same samples to ensure that our observation reflected true nuclear localization, and there was clear staining of the nucleus that co-localized with the GFP fluorescence observed in the nuclei of *GapC1–GFP* and *GapC2–GFP* plants (Supplementary Fig. S1). The quantification of GFP fluorescence intensities revealed significantly fewer fluorescence signals in the nuclei in *des1* background transgenic plants compared with the nuclei in wild-type background plants; furthermore, exogenous sulfide treatment resulted in similar fluorescent signals in nuclei in both wild-type and *des1* plants. These findings were essentially the same in transgenic plants containing both *GapC1–GFP* and *GapC2–GFP* constructs (**Fig. 1I, J**).

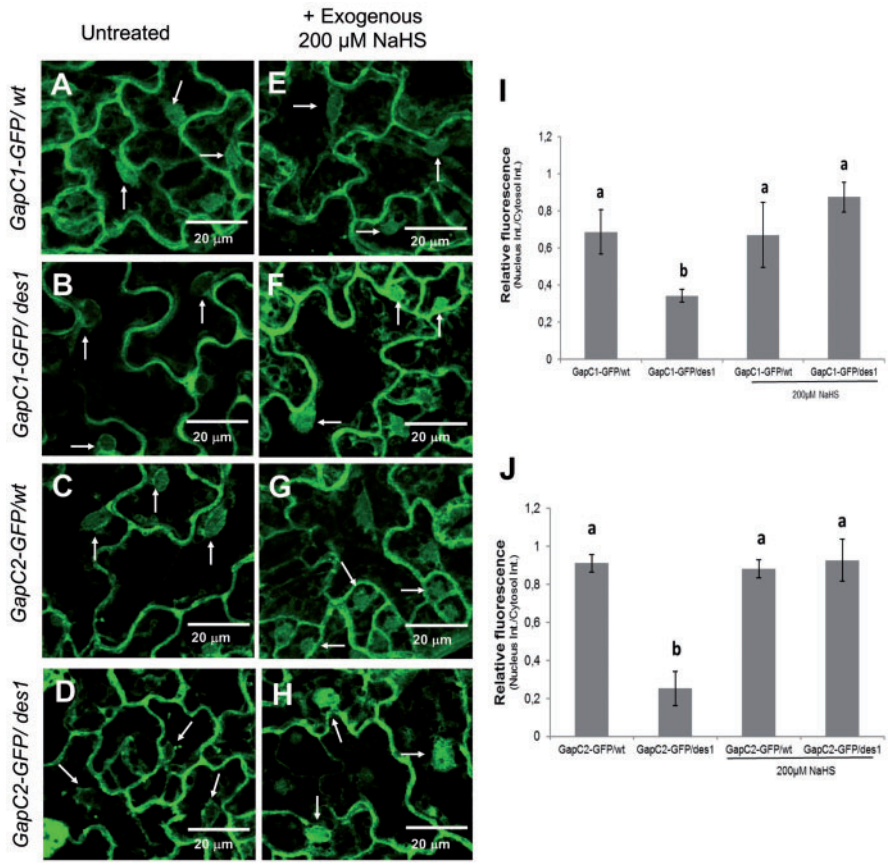

Fig. 1 Effects of sulfide on the subcellular localization of cytosolic GAPDH isoforms. GapC1–GFP- and GapC2–GFP-overexpressing plants on both the wild-type and *des1* backgrounds were grown under physiological conditions. GFP was visualized using confocal fluorescence microscopy in leaves from 30-day-old Arabidopsis plants (A–D) and after 2 h of treatment with 200 µM NaHS (E–H). Arrows indicate nuclei. All images shown are *Z*-stacks of optical sections. GFP fluorescence was assessed using ImageJ software. Values are expressed as relative units ± SD of the fluorescence intensities of nuclei relative to the fluorescence signals in the cytoplasm for GapC1–GFP and GapC2–GFP, respectively (I, J). Different letters indicate significant differences ($P < 0.05$).

To investigate further these results and the effects of sulfide on the translocation of GAPDH cytosolic isoforms at the whole-plant level, we performed subcellular fractionation of the nuclei and cytoplasm from the leaves of 30-day-old wild-type and *des1* mutant Arabidopsis plants grown under physiological conditions or subjected to 15 d of sulfide irrigation as described in the Materials and Methods. GapC protein detection was assessed by immunoblotting with anti-GapC antibodies, either in the enriched nuclear fraction or in the cytosolic fraction (**Fig. 2**). A 37 kDa band of the expected size for GapC proteins was detected in the cytosolic and nuclear fractions in all samples. Two other additional bands were detected in the nuclear fraction, with apparent molecular sizes of 42 and 28 kDa (**Fig. 2A**). The upper band remained constant in all samples and was attributable to cross-reactivity with another nuclear protein. However, the lower band present in the nuclear fraction recognized by anti-GapC significantly increased in intensity when both wild-type and *des1* mutant plants were exogenously treated with sulfide. These results correlate with our observed findings of the effects of exogenous sulfide treatment on GapC–GFP fusion protein localization and suggest that the 28 kDa band may be a processed or post-translationally modified product of the intact GapC proteins. Similar results have previously been observed for the homologous human GAPDH protein, in which a protein band with the same mobility was considered a derived and/or spliced product with unknown functional relevance (Sawa et al. 1997, Yang et al. 2009).

Total amounts of GapC recognized by anti-GapC antibodies in the nuclear extracts were quantified as the sum of immunodetected protein bands (37 + 28 kDa bands) relative to the SYPRO-stained membrane. We observed a 15% reduction in the total amount of GapC in *des1* mutant plants in comparison with wild-type plants, while the total amount of GapC in the cytoplasm remained constant in both treated and untreated samples. In contrast, treatment with exogenous sulfide for 15 d significantly increased GapC protein levels in the nuclei in both wild-type and *des1* mutant plants, specifically the 28 kDa band, with a stronger response to sulfide treatment in wild-type plants. Moreover, the amounts of immunodetected protein bands in *des1* mutants treated with sulfide were significantly higher than those detected in untreated wild-type and *des1* mutant plants (**Fig. 2B**). To estimate the possibility of cytoplasmic contamination in the nuclear extracts during fractionation, we employed antibodies that recognized

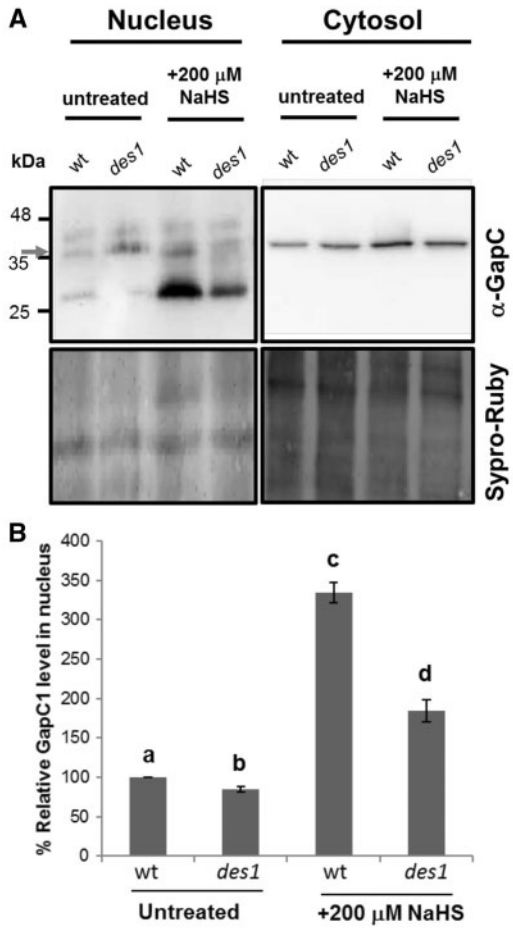

Fig. 2 Hydrogen sulfide mediates GAPDH nuclear accumulation. (A) Western blot analysis of GapC proteins in enriched nuclei and cytosolic extracts. Fifteen-day-old Arabidopsis wild-type and *des1* mutant plants were grown under physiological conditions and irrigated for an additional 15 d in the absence (untreated) or presence of 200 μM NaHS every 4 d. Total protein-enriched nuclei and cytosolic extracts were isolated from leaves and subjected to immunoblot analysis as described in the Materials and Methods. Prior to immunodetection, the membrane was stained with Sypro Ruby as the protein loading control. The arrow marks the expected size of the GapC1 protein (B) Quantification of GapC proteins in the nucleus. Quantification of the sum of immunodetected bands from the enriched nuclear extract with respect to Sypro Ruby staining was performed using Quantity One software. Data shown are the mean ± SD of three independent measures. Analysis of variance (ANOVA) was performed and significant differences are indicated by different letters ($P < 0.05$).

O-acetylserine(thiol)lyase isoform A1 (OASA1) as a cytoplasm-specific subcellular marker. A nuclear envelope protein SUN1,2 antibody (anti-SUN1,2) was used as a nucleus-specific marker to demonstrate the integrity of the nuclear fraction. As shown (Supplementary Fig. S2), OASA1 was detected in the cytoplasmic fraction but not in the nuclear fraction, indicating no contamination of the nuclear fraction by cytosolic proteins. Immunoblotting with the SUN1,2 antibody did not reveal protein degradation in the nuclear fraction. Collectively, our results demonstrate the effects of sulfide on the subcellular localization of GapC proteins and suggest their translocation to the nucleus upon sulfhydration.

To demonstrate the presence of cysteine residues modified by *S*-sulfhydration, we carried out liquid chromatography (LC)–tandem mass spectrometry (MS/MS) analysis on the recombinant GapC1 protein. The digested peptides under non-reducing conditions were analyzed for a 32 Da mass increase in the fragmentation spectrum. Among the peptides identified, SDLDIVSNASC^{156}TTNC^{160}LAPLAK showed a sulfhydryl modification in one of the cysteine residues present, Cys160 according to the protein sequence (**Fig. 3**). To confirm the identification of the 28 kDa nuclear band as GapC1 and the presence of the *S*-sulfhydrated peptide in the nuclear protein, we analyzed by parallel reaction monitoring (PRM) the presence of the *S*-sulfhydrated SDLDIVSNASC^{156}TTNC^{160}LAPLAK peptide identified in the recombinant GapC1 protein and two additional peptides of the GapC1 protein that are lacking cysteine residues, as shown in **Table 1**. As shown in **Fig. 4**, the precursor ion and the fragment ion transitions selected for the peptides VLPALNGK and LVSWYDNEWGYSSR from recombinant GapC1 (**Fig. 4A–E**) were also present in the 37 kDa (**Fig. 4B–F**) and the 28 kDa band (**Fig. 4C–G**). The peak area percentages of the selected ion transitions of both peptides are conserved (**Fig. 4D–H**), therefore confirming the identity of the two protein bands as the GapC1 protein. In addition, using the same technique, we were able to detect the presence of the *S*-sulfhydrated cysteine residue in the 37 kDa and the 28 kDa nuclear bands in the same peptide as the recombinant protein (**Fig. 5**).

Discussion

GAPDH is not simply a classical glycolytic protein; instead, it is a multifunctional protein that demonstrates significant activity in a number of fundamental cell pathways. GAPDH is the prototype moonlighting protein in animal and plant cells, exhibiting activities distinct from its classically identified function in glycolysis, such as DNA stability, control of gene expression, autophagy and apoptosis (Sirover 2014). GAPDH fulfills alternative non-metabolic functions triggered by redox post-translational modifications, such as glutathionylation (Bedhomme et al. 2012), *S*-nitrosylation (Zaffagnini et al. 2013) and cysteine oxidation (Piattoni et al. 2013).

Cytosolic animal GAPDH translocates into the nucleus upon *S*-nitrosylation of the catalytic cysteine residue, which abolishes the glycolytic activity of the enzyme and promotes its binding to the E3-ubiquitin protein ligase, Siah1, causing translocation of the Siah1–NO–GAPDH complex into the nucleus (Sirover 2011). *S*-Sulfhydration of the Cys150 residue of GAPDH enhances its binding to Siah1, and it has been found that *S*-sulfhydration is then followed by *S*-nitrosylation (Mir et al. 2014). Nuclear localization of GAPDH has been characterized in plant systems (Holtgrefe et al. 2008, Vescovi et al. 2013), and interactions with the E3-ubiquitin ligase SEVEN IN ABSENTIA like 7 have been proposed to be responsible for this event (Peralta et al. 2016). However, *S*-nitrosylation does not appear to be the

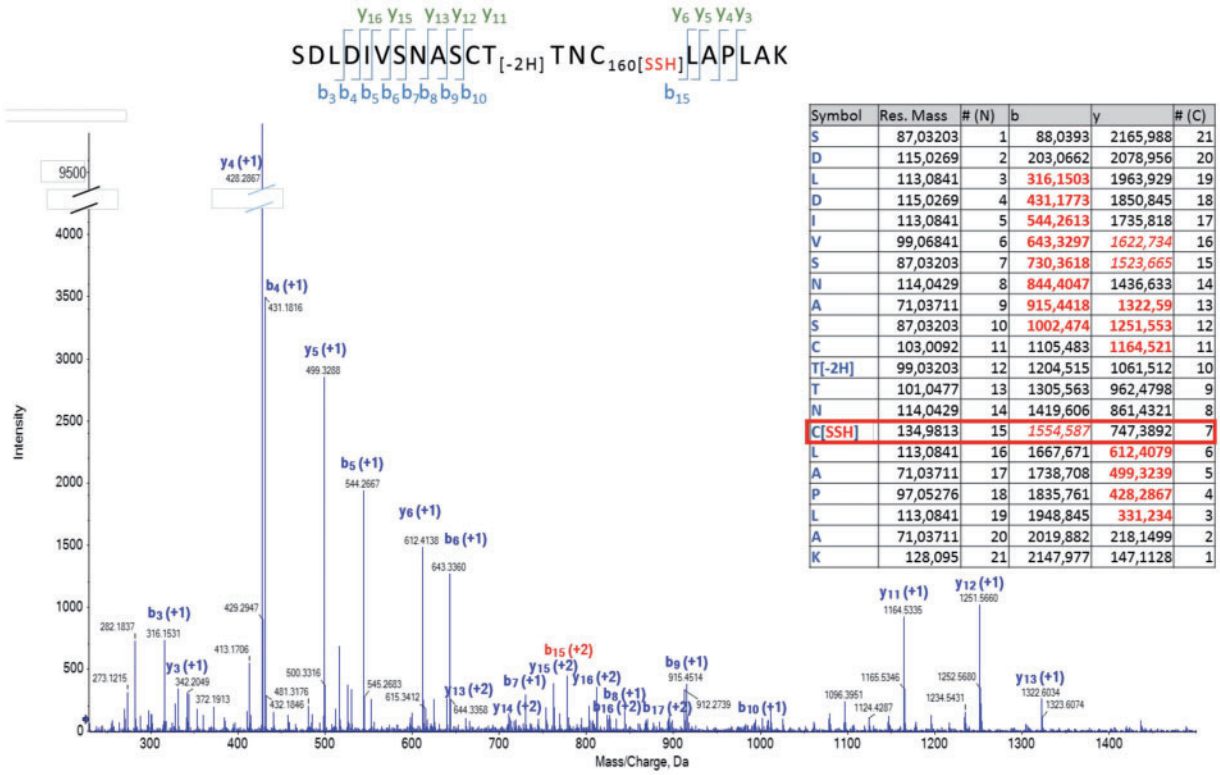

Symbol	Res. Mass	# (N)	b	y	# (C)
S	87,03203	1	88,0393	2165,988	21
D	115,0269	2	203,0662	2078,956	20
L	113,0841	3	316,1503	1963,929	19
D	115,0269	4	431,1773	1850,845	18
I	113,0841	5	544,2613	1735,818	17
V	99,06841	6	643,3297	*1622,734*	16
S	87,03203	7	730,3618	*1523,665*	15
N	114,0429	8	844,4047	1436,633	14
A	71,03711	9	915,4418	1322,59	13
S	87,03203	10	1002,474	1251,553	12
C	103,0092	11	1105,483	1164,521	11
T[-2H]	99,03203	12	1204,515	1061,512	10
T	101,0477	13	1305,563	962,4798	9
N	114,0429	14	1419,606	861,4321	8
C[SSH]	134,9813	15	*1554,587*	747,3892	7
L	113,0841	16	1667,671	612,4079	6
A	71,03711	17	1738,708	499,3239	5
P	97,05276	18	1835,761	428,2867	4
L	113,0841	19	1948,845	331,234	3
A	71,03711	20	2019,882	218,1499	2
K	128,095	21	2147,977	147,1128	1

Fig. 3 LC-MS/MS analysis of the tryptic peptide containing Cys160 of GapC1. The table inside the spectrum contains the predicted ion types for the modified peptide, and the ions detected in the spectrum are highlighted in red.

Table 1 Inclusion list of precursors ions from GapC1

Peptide	Precursor charge	Precursor *m/z*
SDLDIVSNASCT[didehydro]TNC[sulfide]LAPLAK	2+	1,083.4974
SDLDIVSNASCT[didehydro]TNC[sulfide]LAPLAK	3+	722.6674
SDLDIVSNASCT[didehydro]TNCLAPLAK	2+	1,067.5114
SDLDIVSNASCT[didehydro]TNCLAPLAK	3+	712.01
SDLDIVSNASCTTNCLAPLAK	2+	1,068.5192
SDLDIVSNASCTTNCLAPLAK	3+	712.6819
VLPALNGK	2+	406.2554
LVSWYDNEWGYSSR	2+	881.397

T[didehydro], T − 2.01565; C[sulfide] = C + 31.972071.

mechanism responsible for nuclear translocation. Thus, translocation of the GAPDH–NtOSAK (*Nicotiana tabacum* OSMOTIC STRESS-ACTIVATED PROTEIN KINASE) complex to the nucleus is not stimulated by NO treatment (Wawer et al. 2010). Similarly, cadmium treatment induces GapC1 protein accumulation and strong translocation of GapC1 to the nucleus, although translocation is stimulated, rather than inhibited, when the catalytic cysteine of the plant GapC1 is mutated into serine (C155S), excluding *S*-nitrosylation of GapC1 as the mechanism inducing its nuclear translocation (Vescovi et al. 2013).

In a previous study, we provided evidence supporting the regulation of plant GAPDH by *S*-sulfhydration at the catalytic level (Aroca et al. 2015), and, in the present work, we have demonstrated that this modification may determine the cytosolic/nuclear partitioning of this protein. In the Arabidopsis protein, the catalytic Cys156 is *S*-nitrosylated by NO, although the *S*-nitrosylation of GapC1 was excluded as the mechanism inducing its nuclear translocation under cadmium treatment (Vescovi et al. 2013). The translocation can be explained by the sulfhydryl modification of Cys160, as has been determined in this study.

Two different experimental approaches, fluorescence localization of GFP–GapC fusion proteins and immunoblotting, were employed to detect GapC endogenous proteins in enriched nuclear and cytosolic protein extracts, and we obtained similar results from both. We clearly observed a significant reduction in GapC nuclear localization in *des1*-background plants

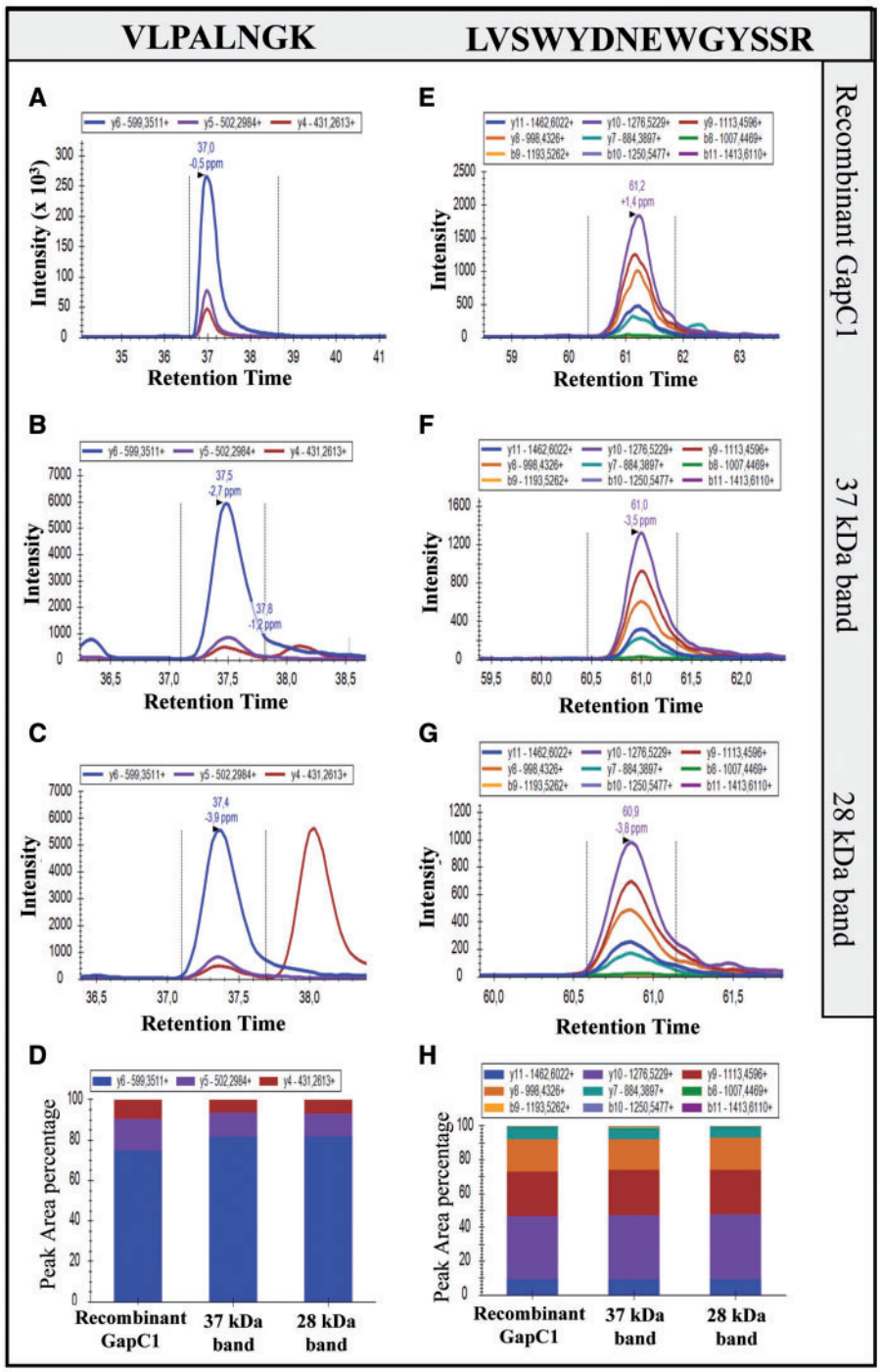

Fig. 4 Identification of the GapC1 protein in nuclear-enriched extract by parallel reaction monitoring. Representative product ions for the precursor ion $[M+H]^{2+}$ at *m/z* 406.25 for the peptide VLPALNGK and for the precursor ion $[M+H]^{2+}$ at *m/z* 881.39 for the peptide LVSWYDNEWGYSSR found in the recombinant protein (A–E), the 37 kDa protein band (B–F) and the 28 kDa protein band (C and G). Peak area percentages for the product ions for both precursors are shown. The contribution from each fragment ion is displayed as a different color in the bars (D–H).

compared with wild-type plants, suggesting that this localization was induced by sulfide treatment, reaching even higher levels of GapC proteins localized in the nucleus in wild-type plants following sulfide treatment. By using a PRM approach, we were able to analyze the presence of the *S*-sulfhydrated peptide SDLDIVSNASCTTNC$^{160}_{[SSH]}$LAPLAK in both the 37 kDa nuclear protein and the lower 28 kDa band. The identification of this apparently processed protein as GapC1 was also confirmed by either immunoblot or the identification of two additional peptides in the protein band by PRM. The fact that the abundance of the 28 kDa isoform was significantly increased after NaHS treatment may suggest that

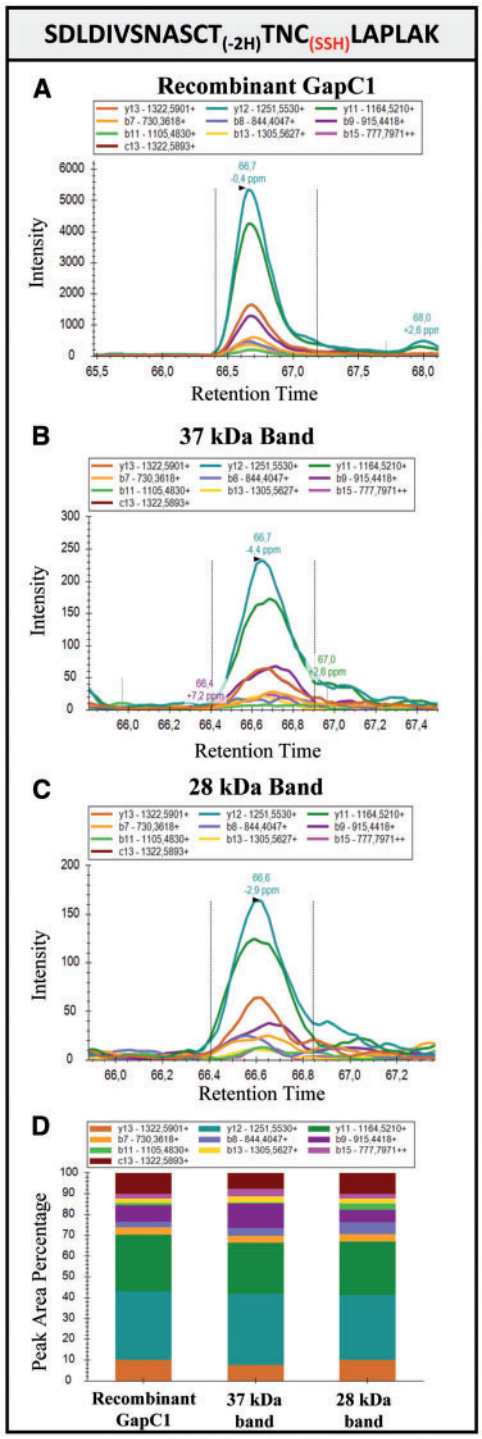

Fig. 5 Identification of the *S*-sulfhydrated peptide SDLDIVSNASCTTNC$_{[SSH]}$LAPLAK in the nuclear-enriched extract by parallel reaction monitoring. Representative product ions for the precursor ion $[M+H]^{3+}$ at *m/z* 722.66 found in the recombinant protein (A) the 37 kDa band from the nuclear extract (B) and the 28 kDa band from the nuclear extract (C). Peak area percentages for each product ion in the three protein samples are shown. The contribution from each fragment ion is displayed as a different color in the bars (D).

S-sulfhydration also influences the stability of the processing of the nuclear isoform, but this aspect will require further study.

The nuclear function of GAPDH in plant systems is not clear, but it probably acts as a coactivator of *NADP-MDH* expression by binding to the *NADP-malate dehydrogenase* (*NADP-MDH*) gene and, consequently, increases the capacity of the malate valve to balance the cellular energy supply (Scheibe 2004, Becker et al. 2006, Hildebrandt et al. 2015).

In conclusion, GAPDH enzyme regulation via S-sulfhydration, both in mammalian cells and in plant systems, appears to be a critical step for reprogramming cellular metabolism via sulfide signaling.

Materials and Methods

Plant material and growth conditions

Arabidopsis (*Arabidopsis thaliana*) wild-type ecotype Col-0 and the *des1* T-DNA insertion mutant (*des1-1*; SALK_103855) were grown in soil under a photoperiod of 16 h of white light (120 μE m^{-2} s^{-1}) at 20°C and 8 h of darkness at 18°C (Bermudez et al. 2012).

To generate the *GapC1–GFP* and *GapC2–GFP* transgenic plants on the wild-type and *des1* backgrounds, the GapC1 (AT3g04120) and GapC2 (AT1g13440) genes were cloned into the pGFP-2 vector as a C-terminal fusion with GFP (Wojtera-Kwiczor et al. 2012). Then, GapC1–GFP and GapC2–GFP were cloned under control of the constitutive 35S promoter into the binary vector pBAR-35S, which contains a Basta (glufosinate) resistance gene. The final transgenic plants were generated via *Agrobacterium tumefaciens*-mediated transformation, and introduction into wild-type and *des1* mutant plants occurred using the floral dip method (Clough and Bent 1998). Plants were selected by Basta resistance, and seedlings were verified by reverse transcription–PCR (RT–PCR). Plants were used for experiments in the F_3 generation.

For immunoblot analysis, 15-day-old plants were irrigated for an additional 15 d with 200 μM NaHS or water every 4 d. For fluorescence experiments, leaves from 30-day-old plants were dipped in 200 μM NaHS or water for 2 h prior to the visualization of GFP fusion proteins by confocal microscopy.

Nuclear protein extraction and immunoblot analysis

Nuclei-enriched and cytosol-enriched extracts were obtained from the 30-day-old wild-type and *des1* Arabidopsis plants following the protocol described (Bowler et al. 2004), with some modifications. Briefly, leaf material (2 g) from untreated and NaHS-treated plants was ground in a mortar under liquid nitrogen and homogenized in 30 ml of Tris–HCl (pH 8) supplemented with 0.4 M sucrose, 10 mM $MgCl_2$ and 0.1 mM phenylmethylsulfonyl fluoride (PMSF). The solution was filtered through a Miracloth layer and then spun for 20 min at 3,200 r.p.m. at 4 °C. The supernatant was removed and kept as the cytosol-enriched extract. The pellet was washed four times with 10 mM Tris–HCl (pH 8) amended with 0.25 M sucrose, 10 mM $MgCl_2$, 1% Triton X-100 and 0.1 mM PMSF, and centrifuged at 2,100×*g* for 10 min at 4°C. The pellet was then disrupted in 400 μl of 20 mM Tris–HCl (pH 8), 150 mM NaCl, 0.1% SDS, 1% Triton X-100 and 2 mM EDTA, followed by sonication for 20 s four times on 30% power with a 550 Sonic Dismembrator for nuclear lysis. Then, samples were spun at 3,200 r.p.m. for 30 s at 4°C, and the pellets were discarded.

The proteins from the nuclei-enriched and cytosol-enriched extracts were separated using non-reducing SDS–PAGE on 12% polyacrylamide gels before transfer to polyvinylidene fluoride membranes (Bio-Rad) according to the manufacturer's instructions. A polyclonal antibody against the cytosolic GAPDH isoform C from the microalga *Scenedesmus vacuolatus*, anti-GapC (Valverde et al. 2005), and secondary antibodies were diluted 1 : 10,000 and 1 : 100,000, respectively. Cytosolic OASA1 and the inner nuclear envelope protein SUN1,2 were used as cell fractionation markers; anti-OASA1 (Alvarez et al. 2011) and anti-SUN1,2 (Agrisera) polyclonal antibodies diluted 1 : 10,000 and 1 : 5,000, respectively, were employed. An ECL Select Western Blotting Detection Reaction kit (GE Healthcare) was used to detect proteins with

horseradish peroxidase-conjugated anti-rabbit secondary antibodies. Prior to immunodetection, the membrane was stained with SYPRO Ruby (Life Technologies) as a protein loading control. The immunodetected protein bands were quantified relative to the SYPRO-stained membrane using Quantity One software (Bio-Rad).

GFP fluorescence analysis

Leaf cells were imaged using a TCS SP2 spectral confocal microscopy (Leica Microsystems), and GFP fluorescence was visualized as described (Gutierrez-Alcala et al. 2005). Light emitted was detected at 510–580 nm. GFP fluorescence was quantified by measuring the integrated GFP signal density and subtracting the background fluorescence using ImageJ 1.37 software. The area and intensity of the nuclei and cytosol were measured. The data represent the average number (±SD) from 10–15 different cells in the analyzed images captured for each experimental condition in three independent experiments.

Fluorescence analysis with SYTO45®

To visualize Arabidopsis nuclei, SYTO® Blue45 Fluorescent Nucleic Acid Stain (Molecular Probes) was used. Leaves were incubated for 15 min under vacuum in a 2 ml solution of purified water amended with 1 µl of SYTO® Blue45 and 0.005% (v/v) Triton X-10. Then, leaf cells were imaged using a TCS SP2 spectral confocal microscope (Leica Microsystems). SYTO® Blue 45 was excited at 458 nm, and emission was detected at 484 nm.

Identification of *S*-sulfhydrated cysteine residues of recombinant GapC1

Recombinant GapC1 protein was obtained as previously described (Aroca et al. 2015). GapC1 was separated using non-reducing SDS–PAGE on 12% (w/v) polyacrylamide gels, and the protein band was excised manually from Coomassie-stained gels, deposited in 96-well plates and processed automatically in a Proteineer DP (Bruker Daltonics). The digestion protocol used was based on Shevchenko et al. (1996) without the reduction or alkylation steps: gel plugs were washed twice, first using 50 mM ammonium bicarbonate and secondly using acetonitrile (ACN), and then dried under a stream of nitrogen (Shevchenko et al. 1996). Then, proteomics-grade trypsin (Sigma-Aldrich) at a final concentration of 16 ng μl^{-1} in 25% (v/v) ACN/50 mM ammonium bicarbonate solution was added, and digestion took place at 37 °C for 5 h. The reaction was stopped by adding 50% (v/v) ACN/0.5% (v/v) trifluoroacetic acid (TFA) for peptide extraction. The tryptic eluted peptides were dried using speed-vacuum centrifugation and were resuspended in 6 microlitres of 0.1% (v/v) formic acid in water. Digested peptides were subjected to one-dimensional nanoliquid chromatography electrospray ionization-MS/MS analysis using a nanoliquid chromatography system (nanoLC Ultra 1D plus; Eksigent Technologies) coupled to a high-speed TripleTOF 5600 mass spectrometer (AB SCIEX) with a duo spray ionization source. Data acquisition was performed using a TripleTOF 5600 System (AB SCIEX). Mass spectrometry and MS/MS data obtained for individual samples were processed using Analyst TF 1.5.1 Software (AB SCIEX). Peptide mass tolerance was set to 25 ppm and 0.05 Da for fragment masses, and only one or two missed cleavages were allowed. Peptides with an individual M_r search score ≥20 were considered correctly identified.

Detection of GapC1 in nuclear extracts by parallel reaction monitoring (PRM)

Recombinant GapC1 protein was obtained as previously described (Aroca et al. 2015) and nuclei-enriched extract was obtained from 30-day-old plants as described above. GapC1 and nuclei-enriched extract were separated using non-reducing SDS–PAGE on 12% (w/v) polyacrylamide gels, and two fractions were excised manually from Coomassie-stained gels from the nuclei sample line around 37 and 28 kDa corresponding to the bands observed by immunoblot. Another band was excised from the recombinant GapC1 line at 37 kDa to be used as a control.

The samples were digested with trypsin without the reduction or alkylation steps. The tryptic-eluted peptides were dried using speed-vacuum centrifugation and were resuspended in 20 µl of 2% ACN and 0.2% TFA. Digested peptides were subjected to one-dimensional nanoliquid chromatography electrospray ionization-MS/MS analysis using a nanoliquid chromatography system (Eksigent nano-LC 415, Sciex) coupled to a high-speed TripleTOF 5600 mass spectrometer (AB SCIEX) with a duo spray ionization source. The trap column was a 25 cm Thermo Acclaim PepMap with 3 µm particle diameter and 75 µm internal diameter, switched online with the analytical column. The nano-pump provided a flow rate of 300 nl min^{-1} and was operated under gradient elution conditions. Peptides were separated using a 60 min gradient ranging from 5% to 30% mobile phase B (mobile phase A, water and 0.1% formic acid; mobile phase B, 100% ACN, 0.1% formic acid). MS/MS data acquisition was performed with a TripleTOF 5600 System (AB SCIEX) using 1 µg of digested recombinant GapC1 and 2 µl of digested nuclei-enriched bands. Samples were subjected to PRM using a 200 ms acquisition time in a mass range of 300–1,200 *m/z* for MS scans, followed by eight MS/MS scans of 200 ms in the mass range of 300–1,500 *m/z* for each ion precursor from the inclusion list (**Table 1**) (total cycle time: 1.85 s). Analysis was performed using Skyline software (v.3.6).

Supplementary data

Supplementary data are available at PCP online.

Funding

This work was supported by the European Regional Development Fund through the Ministerio de Economia y Competitividad [grant No. BIO2013-44648-P] and the Agencia Estatal de Investigación [grant No. BIO2016-76633-P].

Disclosures

The authors have no conflicts of interest to declare.

References

Alvarez, C., Bermudez, M.A., Romero, L.C., Gotor, C. and Garcia, I. (2012a) Cysteine homeostasis plays an essential role in plant immunity. *New Phytol.* 193: 165–177.

Alvarez, C., Calo, L., Romero, L.C., Garcia, I. and Gotor, C. (2010) An O-acetylserine(thiol)lyase homolog with L-cysteine desulfhydrase activity regulates cysteine homeostasis in Arabidopsis. *Plant Physiol.* 152: 656–669.

Alvarez, C., Garcia, I., Moreno, I., Perez-Perez, M.E., Crespo, J.L., Romero, L.C., et al. (2012b) Cysteine-generated sulfide in the cytosol negatively regulates autophagy and modulates the transcriptional profile in Arabidopsis. *Plant Cell* 24: 4621–4634.

Alvarez, C., Garcia, I., Romero, L.C. and Gotor, C. (2012c) Mitochondrial sulfide detoxification requires a functional isoform O-acetylserine(thiol)lyase C in Arabidopsis thaliana. *Mol. Plant.* 5: 1217–1226.

Alvarez, C., Lozano-Juste, J., Romero, L.C., Garcia, I., Gotor, C. and Leon, J. (2011) Inhibition of Arabidopsis O-acetylserine(thiol)lyase A1 by tyrosine nitration. *J. Biol. Chem.* 286: 578–586.

Aroca, A., Serna, A., Gotor, C. and Romero, L.C. (2015) S-sulfhydration: a cysteine posttranslational modification in plant systems. *Plant Physiol.* 168: 334–342.

Becker, B., Holtgrefe, S., Jung, S., Wunrau, C., Kandlbinder, A., Baier, M., et al. (2006) Influence of the photoperiod on redox regulation and stress responses in Arabidopsis thaliana L. (Heynh.) plants under long- and short-day conditions. *Planta* 224: 380–393.

Bedhomme, M., Adamo, M., Marchand, C.H., Couturier, J., Rouhier, N., Lemaire, S.D., et al. (2012) Glutathionylation of cytosolic

glyceraldehyde-3-phosphate dehydrogenase from the model plant Arabidopsis thaliana is reversed by both glutaredoxins and thioredoxins in vitro. *Biochem. J.* 445: 337–347.

Bermudez, M.A., Galmes, J., Moreno, I., Mullineaux, P.M., Gotor, C. and Romero, L.C. (2012) Photosynthetic adaptation to length of day is dependent on S-sulfocysteine synthase activity in the thylakoid lumen. *Plant Physiol.* 160: 274–288.

Bowler, C., Benvenuto, G., Laflamme, P., Molino, D., Probst, A.V., Tariq, M., et al. (2004) Chromatin techniques for plant cells. *Plant J.* 39: 776–789.

Calderwood, A. and Kopriva, S. (2014) Hydrogen sulfide in plants: from dissipation of excess sulfur to signaling molecule. *Nitric Oxide* 41: 72–78.

Clough, S.J. and Bent, A.F. (1998) Floral dip: a simplified method for Agrobacterium-mediated transformation of Arabidopsis thaliana. *Plant J.* 16: 735–743.

Gadalla, M.M. and Snyder, S.H. (2010) Hydrogen sulfide as a gasotransmitter. *J. Neurochem.* 113: 14–26.

Garcia-Mata, C. and Lamattina, L. (2013) Gasotransmitters are emerging as new guard cell signaling molecules and regulators of leaf gas exchange. *Plant Sci.* 201–202: 66–73.

Gotor, C., Alvarez, C., Bermudez, M.A., Moreno, I., Garcia, I. and Romero, L.C. (2010) Low abundance does not mean less importance in cysteine metabolism. *Plant Signal. Behav.* 5: 1028–1030.

Gotor, C., Laureano-Marin, A.M., Moreno, I., Aroca, A., Garcia, I. and Romero, L.C. (2015) Signaling in the plant cytosol: cysteine or sulfide? *Amino Acids* 47: 2155–2164.

Gutierrez-Alcala, G., Calo, L., Gros, F., Caissard, J.C., Gotor, C. and Romero, L.C. (2005) A versatile promoter for the expression of proteins in glandular and non-glandular trichomes from a variety of plants. *J. Exp. Bot.* 56: 2487–2494.

Henry, E., Fung, N., Liu, J., Drakakaki, G. and Coaker, G. (2015) Beyond glycolysis: GAPDHs are multi-functional enzymes involved in regulation of ROS, autophagy, and plant immune responses. *PLoS Genet.* 11: e1005199.

Hildebrandt, T., Knuesting, J., Berndt, C., Morgan, B. and Scheibe, R. (2015) Cytosolic thiol switches regulating basic cellular functions: GAPDH as an information hub? *Biol. Chem.* 396: 523–537.

Holtgrefe, S., Gohlke, J., Starmann, J., Druce, S., Klocke, S., Altmann, B., et al. (2008) Regulation of plant cytosolic glyceraldehyde 3-phosphate dehydrogenase isoforms by thiol modifications. *Physiol. Plant.* 133: 211–228.

Jarosz, A.P., Wei, W., Gauld, J.W., Auld, J., Ozcan, F., Aslan, M., et al. (2015) Glyceraldehyde 3-phosphate dehydrogenase (GAPDH) is inactivated by S-sulfuration in vitro. *Free Radic. Biol. Med.* 89: 512–521.

Kabil, O. and Banerjee, R. (2010) Redox biochemistry of hydrogen sulfide. *J. Biol. Chem.* 285: 21903–21907.

Laureano-Marin, A.M., Moreno, I., Romero, L.C. and Gotor, C. (2016) Negative regulation of autophagy by sulfide is independent of reactive oxygen species. *Plant Physiol.* 171: 1378–1391.

Mir, S., Sen, T. and Sen, N. (2014) Cytokine-induced GAPDH sulfhydration affects PSD95 degradation and memory. *Mol. Cell* 56: 786–795.

Mustafa, A.K., Gadalla, M.M., Sen, N., Kim, S., Mu, W., Gazi, S.K., et al. (2009) H2S signals through protein S-sulfhydration. *Sci. Signal.* 2: ra72.

Mustafa, A.K., Sikka, G., Gazi, S.K., Steppan, J., Jung, S.M., Bhunia, A.K., et al. (2011) Hydrogen sulfide as endothelium-derived hyperpolarizing factor sulfhydrates potassium channels. *Circ. Res.* 109: 1259–1268.

Ortiz-Ortiz, M.A., Moran, J.M., Ruiz-Mesa, L.M., Bravo-San Pedro, J.M. and Fuentes, J.M. (2010) Paraquat exposure induces nuclear translocation of glyceraldehyde-3-phosphate dehydrogenase (GAPDH) and the activation of the nitric oxide–GAPDH–Siah cell death cascade. *Toxicol. Sci.* 116: 614–622.

Paul, B.D. and Snyder, S.H. (2012) H(2)S signalling through protein sulfhydration and beyond. *Nat. Rev. Mol. Cell Biol.* 13: 499–507.

Peralta, D.A., Araya, A., Busi, M.V. and Gomez-Casati, D.F. (2016) The E3 ubiquitin-ligase SEVEN IN ABSENTIA like 7 mono-ubiquitinates glyceraldehyde-3-phosphate dehydrogenase 1 isoform in vitro and is required for its nuclear localization in Arabidopsis thaliana. *Int. J. Biochem. Cell Biol.* 70: 48–56.

Piattoni, C.V., Guerrero, S.A. and Iglesias, A.A. (2013) A differential redox regulation of the pathways metabolizing glyceraldehyde-3-phosphate tunes the production of reducing power in the cytosol of plant cells. *Int. J. Mol. Sci.* 14: 8073–8092.

Romero, L.C., Aroca, M.A., Laureano-Marin, A.M., Moreno, I., Garcia, I. and Gotor, C. (2014) Cysteine and cysteine-related signaling pathways in Arabidopsis thaliana. *Mol. Plant.* 7: 264–276.

Romero, L.C., Garcia, I. and Gotor, C. (2013) L-Cysteine desulfhydrase 1 modulates the generation of the signaling molecule sulfide in plant cytosol. *Plant Signal. Behav.* 8: e24007.

Santo-Domingo, J. and Demaurex, N. (2012) Perspectives on: SGP symposium on mitochondrial physiology and medicine: the renaissance of mitochondrial pH. *J. Gen. Physiol.* 139: 415–423.

Sawa, A., Khan, A.A., Hester, L.D. and Snyder, S.H. (1997) Glyceraldehyde-3-phosphate dehydrogenase: nuclear translocation participates in neuronal and nonneuronal cell death. *Proc. Natl. Acad. Sci. USA* 94: 11669–11674.

Scheibe, R. (2004) Malate valves to balance cellular energy supply. *Physiol. Plant.* 120: 21–26.

Scuffi, D., Alvarez, C., Laspina, N., Gotor, C., Lamattina, L. and Garcia-Mata, C. (2014) Hydrogen sulfide generated by L-cysteine desulfhydrase acts upstream of nitric oxide to modulate abscisic acid-dependent stomatal closure. *Plant Physiol.* 166: 2065–2076.

Shevchenko, A., Wilm, M., Vorm, O. and Mann, M. (1996) Mass spectrometric sequencing of proteins from silver-stained polyacrylamide gels. *Anal. Chem.* 68: 850–858.

Sirover, M.A. (2011) On the functional diversity of glyceraldehyde-3-phosphate dehydrogenase: biochemical mechanisms and regulatory control. *Biochim. Biophys. Acta* 1810: 741–751.

Sirover, M.A. (2014) Structural analysis of glyceraldehyde-3-phosphate dehydrogenase functional diversity. *Int. J. Biochem. Cell Biol.* 57: 20–26.

Takahashi, H., Kopriva, S., Giordano, M., Saito, K. and Hell, R. (2011) Sulfur assimilation in photosynthetic organisms: molecular functions and regulations of transporters and assimilatory enzymes. *Annu. Rev. Plant Biol.* 62: 157–184.

Valverde, F., Ortega, J.M., Losada, M. and Serrano, A. (2005) Sugar-mediated transcriptional regulation of the Gap gene system and concerted photosystem II functional modulation in the microalga Scenedesmus vacuolatus. *Planta* 221: 937–952.

Vescovi, M., Zaffagnini, M., Festa, M., Trost, P., Lo Schiavo, F. and Costa, A. (2013) Nuclear accumulation of cytosolic glyceraldehyde-3-phosphate dehydrogenase in cadmium-stressed Arabidopsis roots. *Plant Physiol.* 162: 333–346.

Wang, R. (2012) Physiological implications of hydrogen sulfide: a whiff exploration that blossomed. *Physiol. Rev.* 92: 791–896.

Waszczak, C., Akter, S., Eeckhout, D., Persiau, G., Wahni, K., Bodra, N., et al. (2014) Sulfenome mining in Arabidopsis thaliana. *Proc. Natl. Acad. Sci. USA* 111: 11545–11550.

Wawer, I., Bucholc, M., Astier, J., Anielska-Mazur, A., Dahan, J., Kulik, A., et al. (2010) Regulation of Nicotiana tabacum osmotic stress-activated protein kinase and its cellular partner GAPDH by nitric oxide in response to salinity. *Biochem. J.* 429: 73–83.

White, M.R. and Garcin, E.D. (2016) The sweet side of RNA regulation: glyceraldehyde-3-phosphate dehydrogenase as a noncanonical RNA-binding protein. *Wiley Interdiscip. Rev. RNA* 7: 53–70.

Wojtera-Kwiczor, J., Groß, F., Leffers, H.-M., Kang, M., Schneider, M. and Scheibe, R. (2012) Transfer of a redox-signal through the cytosol by redox-dependent microcompartmentation of glycolytic enzymes at mitochondria and actin cytoskeleton. *Front. Plant Sci.* 3: 284.

Wu, W. and Berkowitz, G.A. (1992) Stromal pH and photosynthesis are affected by electroneutral K and H exchange through chloroplast envelope ion channels. *Plant Physiol.* 98: 666–672.

Yang, S.H., Liu, M.L., Tien, C.F., Chou, S.J. and Chang, R.Y. (2009) Glyceraldehyde-3-phosphate dehydrogenase (GAPDH) interaction with 3′ ends of Japanese encephalitis virus RNA and colocalization with the viral NS5 protein. *J. Biomed. Sci.* 16: 40.

Zaffagnini, M., Morisse, S., Bedhomme, M., Marchand, C.H., Festa, M., Rouhier, N., et al. (2013) Mechanisms of nitrosylation and denitrosylation of cytoplasmic glyceraldehyde-3-phosphate dehydrogenase from Arabidopsis thaliana. *J. Biol. Chem.* 288: 22777–22789.

Zhang, D., Macinkovic, I., Devarie-Baez, N.O., Pan, J., Park, C.M., Carroll, K.S., et al. (2014) Detection of protein S-sulfhydration by a tag-switch technique. *Angew. Chem. Int. Ed. Engl.* 53: 575–581.